Study of magnetic field enhanced plasma immersion ion implantation in Silicon

2014 J. Phys.: Conf. Ser. 511 012084

(http://iopscience.iop.org/1742-6596/511/1/012084)

Study of magnetic field enhanced plasma immersion ion implantation in Silicon

E J D M Pillaca[1], K G Kostov[1], M Ueda[2]

[1]Dept. of Physics and Chemistry, Faculty of Engineering – FEG, State University of São Paulo – UNESP, Av. Dr Ariberto Pereira da Cunha, 333, Guartinguetá, SP, Brazil

[2]Associated Laboratory of Plasma, National Institute for Space Research, S. J. Campos, SP, Brazil

e-mail: elver_jdd@feg.unesp.br

Abstract. A comparison between experimental measurements and numerical calculations of the ion current distribution in plasma immersion ion implantation (PIII) with external magnetic field is presented. Later, Silicon samples were implanted with nitrogen ion to analyze the effect on them. The magnetic field considered is essentially non-uniform and is generated by two magnetic coils installed on vacuum chamber. The presence of both, electric and magnetic field in PIII create a crossed **E**x**B** field system, promoting drift velocity of the plasma around the target. The results found shows that magnetized electrons drifting in **E**x**B** field provide electron-neutral collision. The efficient ionization increases the plasma density around the target where a magnetic confinement is formed. As result, the ion current density increases, promoting significant changes in the samples surface properties, especially in the surface wettability.

1. Introduction

Plasma immersion ion implantation is a widely used technique for modification material surface properties of complex-shaped three-dimensional (3-D) objects [1]. Basically, the sample to be treated is placed on a sample holder and immersed in plasma and is pulsed to negative high-voltage of several kV. The resultant electric field drives electrons away from the substrate in the time scale of the inverse electron plasma frequency ω_{ep}^{-1} (~ 10^{-9} sec). Thus an ion matrix sheath, which is a region depleted of electrons, forms around the sample holder. The negatively biased substrate will accelerate the ions within a time scale of the inverse ion plasma frequency ω_{ip}^{-1} (~ 10^{-6} sec) towards the substrate and subsequently implant them into the surface. For time order of times ω_{ip}^{-1} the ion flux during the voltage pulse is maitained by the continual expansion of the plasma-sheath edge until it reaches the stationary state for a long time ($t >> \omega_{ip}^{-1}$), where the sheath thickness does not change with the time.
In order to apply the PIII technique successfully to complex-shape workpiece is important to understand the plasma sheath dynamics. Since that sheath dynamics is responsible for the energies distribution of implanted ions several studies on plasma sheaths in PIII has been realized. One of the first to describe the sheath plasma was Langmuir [2]. Due to the importance of the sheath in application such as plasma technology and fusion research there are several works on it [3, 4, 5] and at the present time plasma sheath has received a considerable amount of attention [1]-[21]. A simple one-

dimensional mathematical model was proposed by Lieberman [6] to analyze the sheath expansion in PIII. More realistic situations in PIII considering complex geometry, collision processes, etc. are usually difficult to treat analytically, so numerical methods are required and approaches as fluid model [7], kinetic model [8] and PIC model [9] have been used. There are some observations with respect to the sheath thickness, which if sheath thickness in PIII is not great enough compared with the workpiece size the conformal implantation is not ensured [10]. On the other hand, the sheath thickness should not be too thin (in high pressure) because it can cause electrical breakdown due to very high electrical field strength at the surface [11] [12].
An alternative approach in controlling the sheath thickness is to use a magnetic field. The presence of plasma anisotropy due to the magnetic field does make the analytic treatment very difficult. Consequently a large number of models consider only cases with planar geometry, where the magnetic field intersects the surface target at oblique angles [13][14]. Those studies show that a sheath is significantly affected by the magnetic field. Therefore, it is expected that a magnetic field will affect the sheath dynamics under PIII conditions. Initially, PIII with magnetic fields have been proposed for the suppression of secondary electrons. At the present time, several studies of PIII with external magnetic field have been realized [15][16][17]. On the other hand, the use of strong magnetic field is not desirable in PIII, since it could affect ion trajectories toward the substrate and influence the dose [18].
In this work we analyze the effects caused by the presence of a no-uniform magnetic field in PIII using experimental and numeric techniques. Silicon samples (100) were submitted to PIII treatment with external magnetic field.

2. Experimental and numerical set up

A schematic diagram of the equipment used is shown in figure 1. Cylindrical vacuum vessel of volume ~ 0.02 m^3 is equipped with coils wound on it in order to produces an axial magnetic field. In order to produce the magnetic field the coils are powered by a DC power supply to produce several coil current (I_{coil}). Due to problem of coil heating, the I_{coil} was limited to operate at current below 10 A. Nitrogen plasma is generated by DC glow discharge at pressure ~ $9.4x10^{-3}$ mbar. The procedure is described in detail in [19]. A rectangular steel holder (4x4x16 cm) was built to support Silicon samples (100) on it. It was positioned on the camera axis doing coincides with the center between the magnetic coils. The size of the samples was 1.5x1.5 cm. Before treatment, the samples were ultrasonically cleaned in acetone. The typical treatment parameters were as follow: gas working pressure $9.4x10^{-3}$ mbar, the pulse repetition rate 400 Hz. The pulse voltage was fixed at -3 kV, and the pulse length was 40 μs. The implantation time was 60 minutes.
Before the implantation process the magnetic field inside of the vacuum chamber was mapped using a gaussimeter. The characteristic voltage and current waveforms were recorded using a digital oscilloscope to later investigation. After the implantation process, the Silicon samples were characterized by Atomic Force Microscopy (AFM). A contact angle goniometer (Rame – Hart model 300) was used to measure the water contact angles of the samples in ambient conditions.
To have better insight of the PIII process with magnetic field a numeric simulation was realized. It has been carried out using the computer code KARAT [20]. It employs the particle-in-cell (PIC) algorithm for the calculation of charged particles motion in electromagnetic field. In this simulation we use the 2.5 D computer simulation in cylindrical geometry. Previously, numeric simulation using KARAT code has been used to study the PIII with several configurations of magnetic field [16][17][21] where enhanced of the PIII process was obtained.
KARAT code is implemented with the probabilistic Monte Carlo algorithm to simulate the ionization process. The emission of secondary electrons from the target upon the ion bombardment is also considered in the simulation. In our numerical calculations, rectangular cells with size Δz = 3 mm and Δr = 1.3 mm and a time step of $2.0x10^{-12}$ s were used.
The dimensions of the simulation vacuum chamber as well as the parameters of voltage and gas pressure were close the one experimental parameters described before. The simulation started with an

uniform plasma, $n_i = n_e$, with initial density of $n_o = 5x10^{14}$ m^{-3}, electron temperature $T_e = 3$ eV, ion temperature $T_i = 0$ eV, and secondary electron coefficient of $\gamma = 2.4$ for N^+_2 ions in steel.

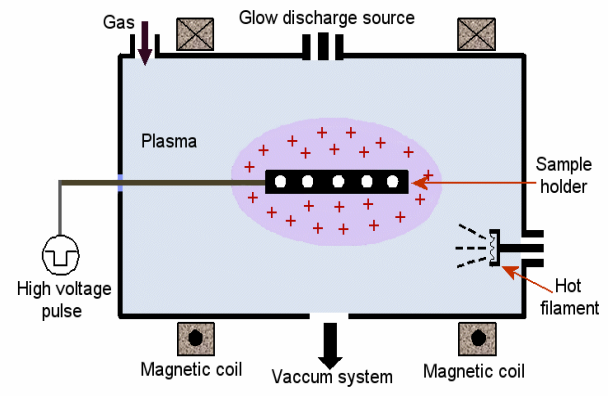

Figure 1. Schematic diagram of PIII vessel.

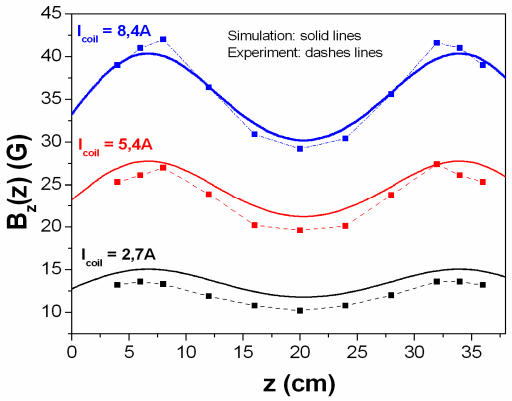

Figure 2. Distribution magnetic field B_z component measured inside of the vacuum chamber.

3. Results and discussions

Figure 2 shows the distribution of the axial magnetic field B_z along the z axis ($r = 0$ cm) produced by I_{coil} of 2.7, 5.3 and 8.4 A. The distribution is not uniform presenting a minimum at $z \sim 20$ cm. That point of symmetry correspond to the center of the target where B_z is weak. This distribution shows two characteristic regions with different amplitude of magnetic field. A minimum value (B_{min}) at $z \sim 20$ cm corresponds to the center between the coils (see figure 1), the maximum values (B_{max}) at $z \sim 7.0$ cm and $z \sim 35$ cm correspond to the coils locations. This configuration is well known as magnetic bottle.

We will define the ratio $R = B_{min}/B_{max}$. Observing figure 2 we can see that for low I_{coil}, $R \rightarrow 1$, that would roughly correspond to an uniform distribution of the magnetic field. The uniformity is lost when $R << 1$, where I_{coil} is high.

The non-uniform static magnetic field showed in figure 2 together with the radial electric field produced by application of the negative voltage to the target creates the system of **E**x**B** crossed field. In this system the behavior of magnetized electrons can be explain in terms of the guiding centre approximation. In presence of **E**x**B** they are accelerated along the magnetic field line [22]:

$$\frac{du_{\parallel}}{dt} = -\frac{\mu_m}{mB}\left[(\mathbf{B}\cdot\nabla)\mathbf{B}\right] \qquad (1)$$

and drifts in the perpendicular direction:

$$u_{\perp} = \frac{\mathbf{E}x\mathbf{B}}{|\mathbf{B}|^2} + \frac{\mu_m}{qB^2}\left[(\nabla B)x\mathbf{B}\right] + \frac{mu_{\parallel}^2}{qB^4}\left[(\mathbf{B}\cdot\nabla)\mathbf{B}\right]x\mathbf{B} \qquad (2)$$

where μ_m, m, q, **E** and **B** denote the magnetic moment, mass of the electron, electric charge, electric field and magnetic field, respectively. The terms of the right hand in (2) are the drift velocity due **E**x**B** fields, the magnetic field gradient drift and magnetic field curvature drift, respectively. Since that the magnitude of the **E**x**B**/**B**^{2} velocity is much larger than the gradient and curvature terms it produces the dominant effect in PIII.

Electrons between two cusps on both sides of the target are reflected in the direction of decreasing magnetic field according to (1), so an axial confinement happen since electrons are reflected from the strong magnetic field regions [17]. Supposing the electric field above the target central region is uniform, then the drift velocity at the fixed radial position is $u_\theta = E/B_z(z)$, where $B_z(z)$ has the axial distribution shown in figure 2.

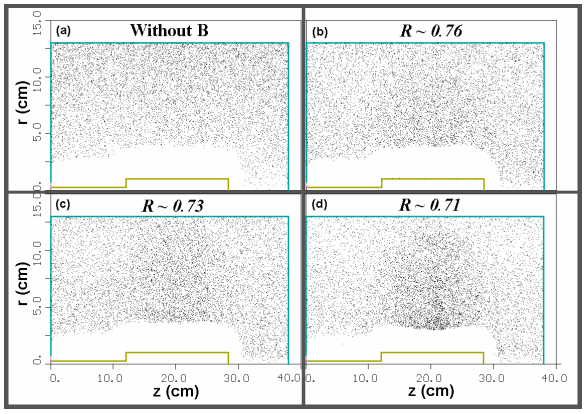

Figure 3. Plasma electron space distribution (a) without magnetic field (c)-(d) with magnetic field at 0.8 μs of simulation time.

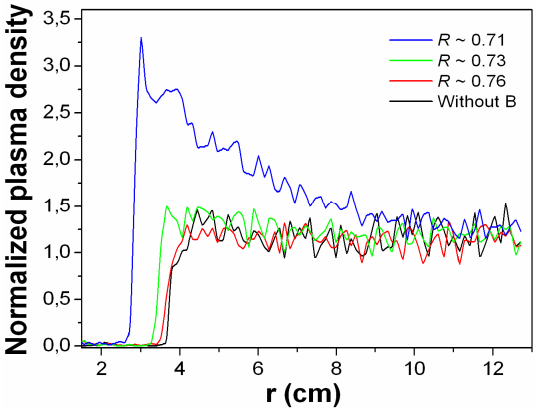

Figure 4. Radial plasma density without and with magnetic field at 0.8 μs of simulation time.

Figure 3 shows the plasma electron space distribution at 0.8 μs of simulation time. The electrons gyrating at azimuthal direction collide with neutrals providing efficient ionization of the background gas. The ionization by magnetization electrons creates a region with high plasma density. As we can deduce from figure 2, the region with high plasma density depends of the B_z distribution, or in other words, depend of ratio R. For low R, the magnetic confinement is more efficient (see figure 3(d)), while at high R the plasma confinement is weaker (see figure 3(b)). The radial plasma density distribution is shown in figure 4. The numeric results show that the plasma density increases by a factor of over two when $R \sim 0.71$. This region is localized between 3 cm to 5 cm radius of at the target middle plane ($z \sim 20$ cm). The growth of the plasma density creates plasma density gradients that affect the dynamics of the sheath (defined as the distance between the target and the plasma edge), reducing it in about 30 % with respects the one without magnetic field. Seeing the figure 2, figure 3 and figure 4 one can perceive that the plasma density growth happens in the region where the magnetic field has minimum value. The plasma sheath edge is also modified in front of target in the case of low ratio R. It can be attributed to the format of the magnetic field distribution over the target. The sheath dynamics as well as the sheath size affect the distribution of implantation current as is shows in figure 5. By decreasing ratio R the dose of implanted ion current onto the target increases, showing a non-uniform distribution at the center.

The relationship between the pulse current waveform and magnetic field was studied. Figure 6 shows the experimental current pulse for different ratios R. The increase of R modifies the current waveform at the characteristic region known as *pulse on*. As we can observe the regions *rise time* and *fall time* remain unaffected. As was previously discussed the increase of the current is attributed to the increase of the plasma density above the target due the efficient ionization of the gas and in presence of magnetic mirror which additionally enhance the process.

Both, experimental and numerical results show an increase of the ion current. It is attributed basically to magnetized electrons that play a key role in the increase of plasma density and consequently in the sheath dynamics. This increase can be predicted by the theory, where the relationship between ion current density and sheath size are related by:

$$j = \frac{4}{9}\varepsilon_0\sqrt{\frac{2e}{M}}\frac{V^{\frac{3}{2}}}{R_t R_s(t)\beta^2} \tag{3}$$

that is the Child-Langmuir law in cylindrical coordinate. Here ε_0 is the free-space permittivity, e is the electron charge, M is the ion mass, R_s and R_t are the sheath and the target radii, respectively, and β is the tabulated function of R_s/R_t.

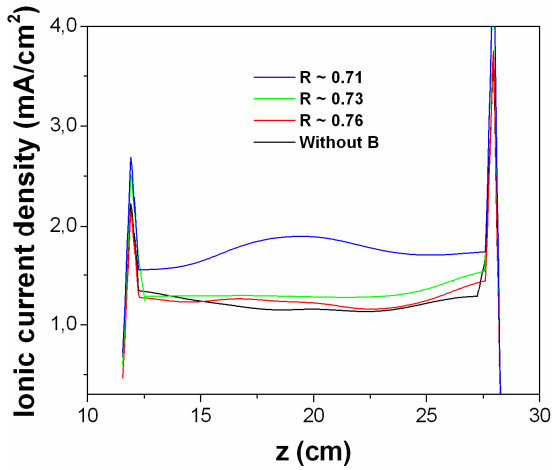

Figure 5. Distribution of ion density current along to target without magnetic field and several ratio R.

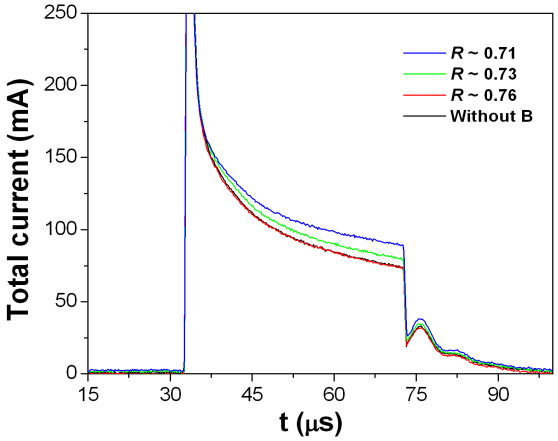

Figure 6. Waveform of the total current without magnetic field and several ratio R.

Silicon samples were implanted with N^+_2 and the results are shown in figure 7, which presents AFM images of a reference sample and samples after implantation process. The scan size of all images was 1x1 μm^2 area. The surface topography is modified when the magnetic field is applied. With the decreases of the ratio R the value of the roughness (R_q) decreases in about 36 % (see table 1) in comparison with the sample treated to case without **B**. This can be attributed to the modification of the ions orbit in presence of **ExB**. Although the ions radius is quite large comparing to the dimension of the vacuum chamber the ion incidence angle onto the surface of the target is influenced by the magnetic field.

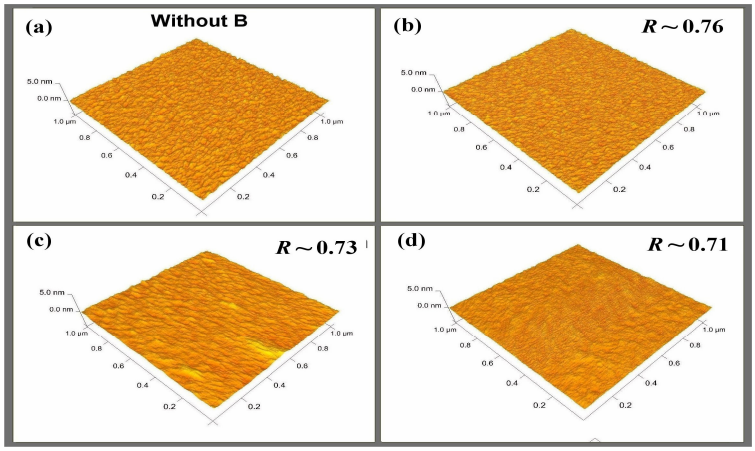

Figure 7. AFM images. (a) Without magnetic field; (b)-(d) with magnetic field.

Table 1. **Values of roughness and water contact angle of Silicon sample**

	Not treated	**Without B**	**R ~ 0.76**	**R ~ 0.73**	**R ~ 0.71**
Rougghness (R_q)	0.26	0.14	0.13	0.11	0.09
Contact angle (^{o})	63.9	83.2	99.8	99.7	99.9

The increase of the ion incident angle would produce more sputtering of the surface as observed in the figure 7(b)-(d). Modification of the roughness leads to modification of the contact angle as is shown in table 1. As we can observe, samples submitted to treatment without magnetic field shows increase in the value of the angle contact in about 31 % with respect the non-treated ones. In presence of the magnetic field this value increases in about 56 % for all the samples. From the increase of the contact angle can be related the different degree of sputtering in the presence of magnetic field. However, further studies are necessary to better understand this relationship.

4. Conclusions

We have presented experimental and numerical results of PIII in the presence of non uniform external magnetic field. We found that plasma density was increased at several *R*. This finding was attributed to collisions between magnetized electrons drifting around the target and neutrals. Numerical results showed that this happens in the region where the magnetic field has minimum value. As a consequence the increase of the plasma density leads to a growth of ion current density. Finally, Silicon samples were implanted and the effects of the magnetic field on their surface properties were analyzed. We found that surface morphology was modified, resulting in higher in roughness and water contact angle. The resulted obtained in this work show that plasma density modification by an external magnetic field with magnetic mirror configuration can have important consequences in the PIII process, as well as in applications in material treatments.

5. References

[1] Conrad J R 1987 *J. Appl. Phys.* **62** 777
[2] Langmuir I 1929 *Phys. Rev.* **33** 954.
[3] Riemann K U 1991 *J Phys. D* **24** 493
[4] Franklin R N 2003 *J. Phys. D* **36** R309
[5] Scheuer J T and Emmert G A 1990 *Phys. Fluids B* **2B** 445
[6] M. A. Lieberman M A 1989 *J. Appl. Phys.* **86** 2926
[7] Gong Y, Wang X, Duan P, Yu J, and Wang 2005 D *Phys. Plasmas* **12** 043501
[8] Scheuer J T and Emmert G A 1988 *Phys. Fluids* **31** 1748.
[9] Briehl B, Urbassek H M 2002 Surface and Coatings Technology **156** 131
[10] Rej D J, Faehl R J, Matossian J N 1997 *Surf. Coat. Techol.* **96** 45
[11] Anders A 2000 *Appl. Phys. Lett.* **76** 28
[12] Keidar M 2006 *IEEE Transactions on Plasma Science* **34** 804
[13] Ahedo E 1997 *Phys. Plasmas* **4** 4419
[14] Masoudi S F, Esmaeili S S, Jazavandi S 2010 *Vacuum* **84** 382
[15] Ueda M, Tan I H, Dallaqua R S, Rossi J O 2007 Surf. Coat. Technol. **201** 6597
[16] Kostov K G and Barroso J J 2006 IEEE Transactions on Plasma Science **34** 1127
[17] Kostov K G, Algatti M A, Pillaca E J D M, Kayama M E, Mota R P, and Honda R Y 2009 *Eur. Phys. J. D* 205
[18] Tan I H, Ueda M, Oliveira R M, Dallaqua R S, Reuther H 2007 Surf. Coat. Technol. **201** 4826
[19] Ueda M, Berni A, and Gomes G F, Beloto A F and Abramot E 1999 *J. Appl. Phys.* **86** 4821
[20] Tarakanov V P 1994 *User's Manual for Code KARAT* Berkeley VA: Berkeley Res. Assoc. Inc.
[21] Kostov K G, Barroso J J, and Ueda M. 2004 *Brazilian Journal of Physics* **34** 4B
[22] Schmidt G 1979 *Physcs of High Temperatur Plasma* second edition Academic Press INC